Bioprocess and Biosystems Engineering (2019) 42:1023–1037
https://doi.org/10.1007/s00449-019-02102-z

RESEARCH PAPER

Application of process system engineering tools to the fed-batch production of poly(3-hydroxybutyrate-*co*-3-hydroxyvalerate) from a vinasses–molasses Mixture

Cesar García[1,2] · Wilman Alcaraz[2] · Alejandro Acosta-Cárdenas[2] · Silvia Ochoa[1]

Received: 14 November 2018 / Accepted: 3 March 2019 / Published online: 14 March 2019

Abstract
Fed-batch production of poly(3-hydroxybutyrate-*co*-3-hydroxyvalerate) copolymer using vinasses–molasses mixture is carried out in this work by implementing different process systems engineering tools. Two fed-batch strategies are tested experimentally at 5 L scale, considering only offline information: (1) offline optimizing control and (2) exponential feeding. Application of these strategies showed that different feeding profiles result in different dynamic behaviour, influencing both, yield and biopolymer properties. As offline-based feeding strategies do not consider information of the culture status, they cannot deal with uncertainties. Therefore, a closed loop control strategy was implemented, which uses biomass and substrate information predicted online by soft-sensors. Results demonstrated the technical feasibility to produce biopolymer using a 75/25%vol. vinasses–molasses mixture. Successful implementation of the soft-sensor-based control strategy was evidenced at pilot plant scale, where sugar concentration was kept almost constant for 14 h, while obtaining the desired copolymer. Thus, proposed control strategy could be of interest at industrial-scale.

Keywords Fed-batch culture · Soft-sensor · Polyhydroxyalkanoates · Closed loop control · Vinasses · Molasses

Introduction

Polyhydroxyalkanoates (PHAs) are polymers of biological origin, claimed to be an environmentally friendly option for replacing petroleum-based plastic materials in a wide number of applications. However, production costs of these materials are still higher when compared to petroleum-based plastics, preventing the expansion of this biopolymer industry, in spite of its innumerable environmental advantages. Therefore, in the past years, many efforts from the academic field have been done in order to improve the technical and economic feasibility of the process [1]. Some of these efforts have focused on using alternative low-cost substrates [2–5]. Other works have focused on using tools from the process systems engineering (PSE), in order to address the modelling, optimization and control of the process, towards increasing its productivity [6–10]. Recently, some references [4, 5] have reported the use of vinasses as low-cost substrate for producing PHA-type biopolymers, which is attractive in terms of using such kind of waste for obtaining a high valuable product. The main interest on exploring the use of vinasses is that they are a residual liquid obtained in very high amounts as by-product of the ethanol industry. As an example, the sugarcane-based bio-ethanol industry generates around 10–15 litres of vinasses per litre of ethanol produced [11]. This means that only in Brazil, which is the largest ethanol producer from sugarcane worldwide, between 2011 and 2012, 492.70 million tons of sugarcane were processed, producing 12.7 billion litres of hydrated ethanol and 190.7 billion litres of vinasses [12]. Vinasses are commonly used as fertilizer and soil conditioner in sugar cane fields [11, 13], and although they are not considered a hazardous waste, they are indeed a complex recalcitrant wastewater. Therefore, their discharge into the environment can contaminate the soil and groundwater [11], which is a serious environmental concern, especially when considering the high amount of vinassses produced worldwide. Therefore, it is important to explore alternatives for using such wastes and convert them

✉ Silvia Ochoa
silvia.ochoa@udea.edu.co

[1] SIDCOP Research Group, University of Antioquia, Medellín, Colombia

[2] Biotransformación Research Group, University of Antioquia, Medellín, Colombia

into higher value-added products. In this direction, vinasses have been used for biogas production [14] and for PHA production [4, 5]. In the case of PHAs obtained from vinasses, production of PHA biopolymers has been reported by *Haloarcula marismortui* [4] and *Haloferax mediterranei* [5]. The former work reported that obtained PHA was very similar to the standard poly(3-hydroxybutyrate) (P3HB) from Sigma, whereas the latter reported obtaining the co-polymer poly-3-(hydroxybutyrate-*co*-hydroxyvalerate). Furthermore, production of poly(3-hydroxybutyrate) by *Cupriavidus necator*, using as raw material a mixture of cane molasses and vinasses has been recently reported by Acosta-Cárdenas et al. These authors found that the most suitable proportion of molasses/vinasses mixture was 25/75%vol [15]. As it has been reported, vinasses are characterized by their low pH, dark brown color and high content of ashes and dissolved organic and inorganic matter [16]. It is important to notice that vinasses also contain a considerable number of inorganic salts (i.e. sulfates, phosphates). Precisely, this high salt content allows carrying out the PHA production without supplementing additional nutrients. Therefore, producing PHAs by using vinasses has two main advantages: (1) costs related to nutrients and raw materials are reduced and, (2) giving a different use to such waste would reduce the environmental impact caused by the bioethanol industry.

Production of PHAs using a vinasses–molasses mixture is carried out in this work in batch and fed-batch operation. As it is known, an important fact in fed-batch fermentations is the definition of the feeding strategy. Different strategies have been reported in the literature for calculating the feeding profile of nutrients in fed-batch fermentations [17]. The work in Ref. [18] shows an excellent review on the topic of control strategies for manipulating the feed rate in fed-batch fermentation processes. Although academic developments in this field go up to the use of the model-based predictive control (MPC) strategy, it can be noticed that at industrial level, carbon-limited fermentation processes are still operated following any open loop strategy [19]. There are two main reasons for this: (1) additional investment costs for implementing a closed loop control strategy are required (hardware and software) and (2) the absence of reliable online measurements for key process variables: biomass, substrate and metabolite concentrations. These reasons prevent the application of closed loop control strategies to fed-batch fermentations at industrial level and, therefore, open loop control is the current approach [18, 20]. Open loop control applies a predefined feeding profile, which is calculated taking into account the initial process conditions and the defined operating point, without using any information of the actual process state. Therefore, although less expensive, open loop control is not able to reject disturbances to the system, which is one of the reasons of the variability observed from batch to batch in bioprocesses.

This work is directed to contribute towards the improvement of the technical and economic feasibility of the biopolymers industry, by using a vinasses-molasses mixture as low-cost raw material (impacting the process economy) and by implementing Process Systems Engineering tools (i.e. modelling and control) for improving the process performance. Some species of bacteria that produce Polyhydroxyalkanoates, such as *Cupriavidus necator, Azohydromonas australica* and recombinant *Escherichia coli*, have been used for producing this type of bio-polymers at industrial scale [21]. Following previous results reported in reference [15], a mixture of vinasses and molasses in a ratio 75/25%vol., respectively, is used for producing PHAs by *Cupriavidus necator* ATCC 17699. For controlling the process, two open loop strategies are compared: an offline optimizing control strategy and the commonly used exponential feeding strategy. As it will be shown, using these two different feeding strategies has led to obtain biopolymers with different characteristics. Furthermore, it was observed that operating the process in an open loop strategy is not optimal at all. Therefore, a closed loop strategy is proposed which relies on the use of soft-sensors that only require online measurement of O_2/CO_2 at the exhaust gas.

Materials and methods

In this study, the fermentation of sugars present in a vinasses-molasses mixture by *Cupriavidus necator* ATCC 17699 to produce PHBV has been carried out at 5 L and 500 L scale. Both bioreactors are stirred tanks and have the same geometrical similarity.

Pre-treatment of vinasses

Vinasses used in this study were obtained from a Colombian sugarcane factory located in the Valle del Cauca region, which produces ethanol from sugarcane molasses. The vinasses were stored in a freezing room at 4 °C. Based on a previous work [15], a mixture of vinasses and molasses (75/25%vol. respectively) was prepared in order to obtain an initial total sugars (i.e. fructose, glucose and sucrose) concentration of ~ 20 g/L. Before fermentation, the mixture of vinasses–molasses was heated at 80 °C for 6 h. Afterwards, the pH was adjusted to 3.5. This process was performed in order to sterilize the medium and to precipitate organic wastes.

Strain and cultivation conditions

Cupriavidus necator ATCC 17699 was purchased from ATCC (Manassas, VA, USA) through CES University (Medellín, Colombia). They remained cryopreserved at

− 20 °C in TSB medium (formula per Liter Purified Water: Tryptone 17.0 g, Soytone 3.0 g, Glucose 2.5 g, Sodium Chloride 5.0 g and Dipotassium Phosphate 2.5 g) and 30% glycerol in 1.5 mL vials. The inoculum used for the reactor culture was prepared in 1 L Erlenmeyer flasks with a volume of TSB medium corresponding to 10% of the reactor working volume. Vials containing the cryopreserved cells were taken and brought to room temperature. Then, it was inoculated in TSB medium and incubated in a shaker at 30 °C and 150 rpm for 12 h. The culture medium used is a combination of sugarcane vinasses–molasses in a ratio 75/25%vol, respectively, as suggested by Ref. [15]. Batch experiments were carried out in a 5 L New Brunswick BioFlo/CelliGen 115 bioreactor. The open loop fed-batch experiments were carried out in the same reactor as the batch experiments. The proposed closed loop strategy for the fed-batch fermentations was implemented in a 500-L fermentor located at the Microbiology School at Universidad de Antioquia (Medellín, Colombia). All experiments included pH, temperature and dissolved oxygen control at 7, 30 °C and 40%, respectively.

Analytical methods

Samples for cell dry mass, polymer and sugars quantification were taken every four hours. Cell dry mass (CDM) was determined using a 1-ml culture which was centrifuged in a 1.5-mL vial for 10 min at 4722*g*. The supernatant was decanted into a new tube and stored in a freezer for subsequent sugars analysis. The vial containing the sediment was refilled with 1 mL distilled water for a second centrifugation. The second supernatant was discarded and the pellet was suspended in distilled water and poured into a pre-weighed vial. The tube was placed in an oven at 80 °C for 12 h (until constant weight) in order to determine biomass concentration [5]. For the analysis of the sugars, high-performance liquid chromatography (HPLC) Agilent Technologies 1200, model 61362A, with an ionic separation column Animex HPX-87H, 300 × 7.8 mm was used. Samples were centrifuged at 3615*g* for 5 min and aliquots of the supernatant were taken, which were diluted in mobile phase (sulfuric acid 0.008 N). Each diluted sample was run through 0.2 µm regenerated cellulose filters and injected under the following conditions: 20 µL sample, 0.6 mL/min flow, 35 °C and 12 min run time. All samples were analysed in triplicate. For the PHA quantification, a solvent extraction protocol was used as follows [22, 23]: Samples were centrifuged at 5331*g* and 30 °C for 10 min. Biomass recovered was mixed with a hypochlorite (15%)–chloroform solution (2:1 ratio), at 30 °C, 120 rpm during 90 min, in shaker. The mixture was left in repose overnight and three phases were formed: hypochlorite, cellular debris and chloroform with dissolved polymer. The phase containing the chloroform with dissolved polymer was decanted and separated by rotoevaporation. Finally, the polymer was dried in an oven at 60 °C for 12 h and was weighed in analytical balance.

Polymer characterization

For characterizing the molecular structure and functional groups present on the obtained polyhydroxyalkanoate, Fourier transform infrared spectroscopy (FTIR) was used. Samples were characterized in a spectrometer Shimadzu-Affinity-1, by using KBr pellets in the range of 400–4000 cm^{-1} at a spectral resolution of 4 cm^{-1}, where 15 scans per run were used. The obtained spectrum was compared with a commercially available PHBV standard from Sigma (Poly(3-hydroxybutyric acid-*co*-hydroxyvaleric acid), natural origin, PHV content 12 mol %- CAS number: 80181-31-3). Differential Scanning Calorimetry (DSC Q100 from TA Instruments) was used for determining the thermal characteristics of the produced polymer. A standard method was adopted following the next described temperature program: samples were heated from environmental conditions (25 °C) up to 200 °C at a rate of 50°C/min. At 200 °C, temperature was kept constant for 2 min. Then, it was cooled to − 80 °C at a rate of − 20 °C/min, keeping this temperature for two minutes. Finally, the sample was heated again up to 200 °C at a rate of 10°C/min. The melting peak (T_m) and the glass transition temperature (T_g) were obtained from the second heating ramp. Additionally, NMR was used for the determination of the polymer structure. The NMR was carried out using a Bruker equipment (Ascend III HD 600 MHz) with deuterated chloroform as solvent. The obtained polymer was identified as a co-polymer P(3HB-co-3HV). Determination of the 3-hydroxyvalerate (3HV) content was carried out using Eq. (1), where area CH_3(3HV) denotes the area under the peaks at 0.79 ppm (corresponding to the absorption of the methyl group from the 3-hydroxyvalerate), whereas area CH_3(3HB) denotes the area under the peaks corresponding to 1.2 ppm [absorption of the methyl group from the 3-hydroxybutyrate (3HB)]:

$$\%3\mathrm{HV} = \frac{\text{area } CH_3\ (3\mathrm{HV})}{\text{area } CH_3\ (3\mathrm{HV}) + \text{area } CH_3\ (3\mathrm{HB})} \times 100\%. \quad (1)$$

Results and discussion

Fed-batch open loop control strategy at 5 L

In this section, results obtained when applying open loop control by using two different strategies (1) offline optimizing control and, (2) exponential feeding, are compared. Since the optimizing control approach requires a model of the process in order to be implemented, the model used is introduced first.

Then, a comparison between the applied open loop control strategies is shown.

Unstructured model

The developed model is based on the works by Amicarelli et al. [24] and Chatzidoukas et al. [25]. The model is described by Eqs. (2–8), where the dynamic equations describing the behaviour of the biomass (X), substrate (S) (as total sugars, i.e. fructose, glucose and sucrose in the vinasses-molasses mixture), biopolymer (P), nitrogen-source (N), dissolved oxygen (O_{2L}) and the volume are given. The specific growth rate (μ) is a function of carbon/nitrogen ratio and the dissolved oxygen concentration, following a sigmoidal relationship. F and F_{air} correspond to the feed flow rate of the substrate (sugars in the vinasses–molasses mixture) and air, respectively. S_{in} and N_{in} correspond to the sugars and nitrogen concentrations at the feed. Finally, V is the fermentation volume. Model parameters are described in Table 1.

$$\mu = \mu_m \left[\frac{\left(\frac{N}{S}\right)}{\left(\frac{N}{S}\right) + K_{sr}} \right] \cdot \left[1 - \left(\frac{\left(\frac{N}{S}\right)}{S_m} \right)^{n_k} \right] \cdot \left[\frac{O_{2L}}{K_{ox} X + O_{2L}} \right], \tag{2}$$

$$\frac{dX}{dt} = \mu X - \frac{F}{V} X, \tag{3}$$

$$\frac{dS}{dt} = -C_{sx} \mu X - R_{csx} X - C_{sp} \left(K_1 \mu X + K_2 X \right) + \frac{F}{V} \left(S_{in} - S \right), \tag{4}$$

$$\frac{dP}{dt} = K_1 \mu X + K_2 X - \frac{F}{V} P, \tag{5}$$

$$\frac{dN}{dt} = -C_{nx}\, \mu X - R_{cnx} X + \frac{F}{V} \left(N_{in} - N \right), \tag{6}$$

$$\frac{dO_{2L}}{dt} = \frac{F_{air}}{V} O_{2,loeq} + K_L \left(O_{2Leq} - O_{2L} \right) - \mu X O_{2L} \left(K_3 + K_1 K_4 \right) - K_2 K_4 X O_{2L} - \frac{F}{V} O_{2L}, \tag{7}$$

$$\frac{dV}{dt} = F\,. \tag{8}$$

First three terms in Eq. (4) consider substrate consumption due to biomass synthesis, maintenance and polymer production, respectively. Polymer production is represented by the first two terms in Eq. (5), accounting for a growth-associated and a non-growth-associated terms, respectively. Nitrogen-source dynamic behaviour represented by Eq. (6) *considers nitrogen consumption* due to biomass synthesis and maintenance. Finally, Eq. (7) shows the dynamic for the dissolved oxygen concentration where mass-transfer limitation phenomena have been negligible. The oxygen uptake rate is calculated as the contribution of the oxygen consumption rate for residual biomass growth/and maintenance (third term), and for polymer production in the cells (fourth term) [25]. The model contains 16 parameters. For identifying those parameters, a hybrid strategy combining the simulated annealing and the interior point method was used. The objective function for parameter identification is given by Eq. (9).

$$\mathrm{SSWR} = \sum_{i=1}^{n} \sum_{j=1}^{m} \frac{\Delta_{ij}}{W_j^2}, \tag{9}$$

where SSWR represents the sum of squared weighted residuals, n and m are the total number of experimental data points

Table 1 Parameters for the unstructured model

Symbol	Description	Value
μ_m (h^{-1})	Maximum specific growth rate	0.803 ± 0.078
K_{sr}	Saturation constant	6×10^{-5}
n_k	Dimensionless exponent	5.01 ± 3.822
S_m (gN/gS)	Maximum value of substrate at which complete inhibition occurs	0.011
K_{ox} (gO_2/gX)	Oxygen limitation constant	0.00118
C_{sx} (gS/gX)	Consumption coefficient for residual biomass synthesis	2.066 ± 0.772
R_{csx} (gS/gX h)	Substrate consumption rate for maintenance	0.00837
C_{sp} (gS/gP)	Consumption coefficient for polymer production	1.559 ± 2.081
K_1 (gP/gX)	Yield of product respect to biomass	0.028 ± 0.036
K_2 (gP/gX h)	Product consumption rate	0.045
C_{nx} (gN/gX)	Nitrogen-source consumption coefficient for residual biomass synthesis	0.14792 ± 0.073
R_{cnx} (gN/gX h)	Nitrogen-source consumption rate for maintenance	0.209 ± 0.165
K_L (h^{-1})	Aeration constant	0.05313 ± 0.05
K_3 (L/gX)	Kinetic constant	76.421 ± 0.533
K_4 (L/gP)	Kinetic constant	55.268 ± 26.866
$O_{2,loeq}$ (g/L)	Dissolved oxygen concentration at saturation	0.002 ± 0.001

and variables, respectively. W_j is a normalization factor for each variable. Δ_{ij} is the difference between the predicted and experimental data. The estimated model parameters are given in Table 1. Figure 1 shows a comparison between the model predictions and the experimental data taken during fed-batch operation following the feeding profile given in Fig. 1d. As it can be observed, model predictions are in good agreement with the experimental data.

Experimental results for open loop control: offline optimizing control vs. exponential feeding

As it was mentioned, two open loop control strategies were implemented in order to compare their effect on the process dynamic behaviour and on the characteristics of the final obtained polymer. For implementing the offline optimizing control, a Dynamic Optimization (Dyopt) problem was solved in order to calculate the feeding profile required for increasing the process productivity, while fulfilling the constraints. For solving the Dyopt problem, the control vector parameterization approach was used [26]. A piecewise constant parameterization for the feed flow rate was used, which is described by Eqs. (10–11).

$$F = \sum_{j=1}^{m} a_{\text{iok}} \varphi\left(t_{i-1}, t_i\right)\left(u_{\max} - u_{\min}\right) + u_{\min}, \tag{10}$$

$$\varphi\left(t_{i-1}, t_i\right) = \begin{cases} 0, & t < t_{i-1} \\ 1, & t_{i-1} \le t < t_i \\ 0, & t \ge t_i \end{cases}, \tag{11}$$

where $m = 6$ is the number of steps pre-defined. $u_{\max}$ and $u_{\min}$ correspond to the maximum and minimum values for each step (magnitude of each step in L/h). The a_{iok} is the vector

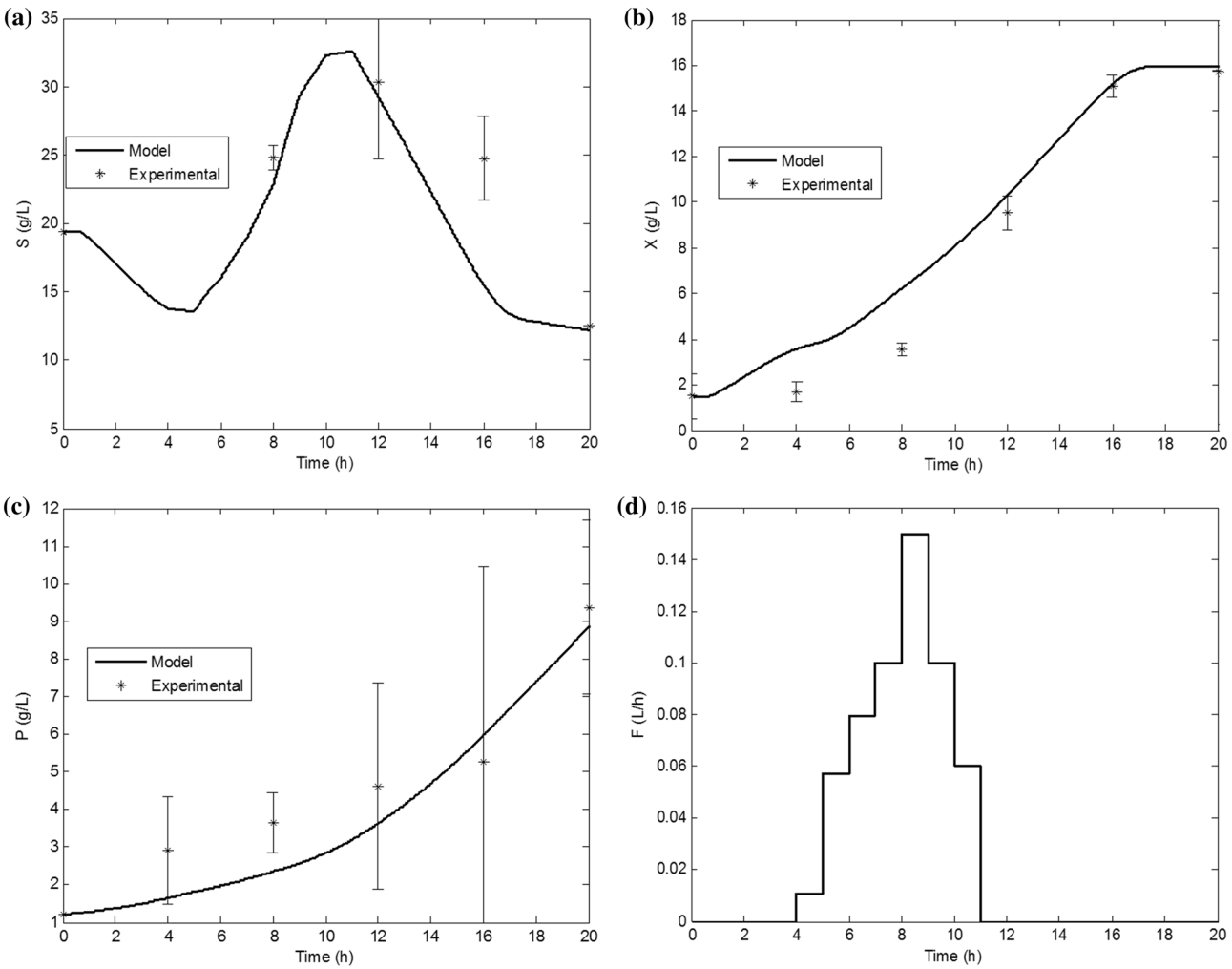

Fig. 1 Comparison: Unstructured model predictions vs. experimental data for fed-batch PHA production at 5 L scale. Results for the main state variables: **a** substrate, **b** biomass, **c** polymer concentration and **d** feeding profile

of parameters that defines the control vector profile, and is, therefore, the vector of decision variables of the Dyopt problem.

The dynamic optimization (Dyopt) problem is described in Eq. (12):

$$\underset{F(t)}{\text{Maximize}} \quad P(t_f) \cdot V(t_f), \tag{12}$$

$$\text{s. to.} \quad 0 \le F \le 1 \quad \left[\frac{L}{h}\right], \tag{12a}$$

$$\max S(t) \le 30 \left[\frac{g}{L}\right], \tag{12b}$$

$$V \le 5L, \tag{12c}$$

$$\frac{d\boldsymbol{x}}{dt} = f(\boldsymbol{x}, F), \tag{12d}$$

where t_f is the final process time. Constraint (12a) denotes the maximum and minimum values allowable for F. Constraint (12b) imposes an upper limit for the substrate concentration, in order to avoid inhibition, whereas constraint (12c) restricts the maximum working volume. Finally, constraint (12d) represents the model Eqs. (2)–(8).

On the other hand, for applying the exponential feeding strategy, Eq. (13) was used.

$$F(t) = \begin{cases} \alpha_1 \alpha_2 e^{\alpha_2 t}, & t_0 \le t \le t_f \\ 0, & \text{otherwise} \end{cases}, \tag{13}$$

where

$$\alpha_1 = \frac{X_0 V_0}{S_{\text{in}} Y_{X/S}}, \tag{14}$$

$$\alpha_2 = \mu. \tag{15}$$

The exponential feeding profile is assumed to allow cells to grow at a constant specific growth rate [27]. X_0 and V_0 represent the biomass concentration and the volume at the beginning of the fed-batch phase, respectively. S_{in} is the substrate concentration in the feed stream. $Y_{X/S}$ is the cell yield on substrate, whereas μ is the desired specific growth rate for the microorganism. Table 2 shows the experimentally determined parameters (from previous batch experiments) used in the calculation of the exponential feeding profile.

Figure 2 compares the experimental results obtained for the fed-batch production of PHAs from the vinasses–molasses mixture when applying the two described feeding profiles. Furthermore, for the sake of comparison, batch experimental results are also shown.

As it can be seen in Fig. 2, the fed-batch-optimizing control strategy resulted in the highest polymer concentration by using the carbon source in a more efficient way (the exponential strategy resulted in highest substrate accumulation). Table 3 summarizes the results of applying the three different fermentations strategies, in terms of the reaction yield, product yield, productivity and maximum PHA content obtained during 24 h of total operation. As it can be seen, the fed-batch optimizing control strategy resulted in the highest reaction yield (mass of polymer produced per mass of substrate added to the reactor), highest PHA content and highest productivity. However, the attained product yield obtained (mass of polymer produced per mass of substrate consumed by the microorganism) is not satisfactory. Furthermore, the fed-batch-exponential strategy resulted in the lowest reaction yield (even lower than the batch), showing that this strategy is not suitable at all. Therefore, it is clear that the yield (both the reactor and product yields) and the productivity must be improved in order to really claim the advantages of fed-batch operation over batch for the case analysed.

Table 2 Parameters for calculating the exponential feeding profile

Parameter[a] (units)	Value
Yx/s (gX/gS)	0.38
μ (h^{-1})	0.15
Vo (L)	2.5
Xo (gX/L)	1.41

[a]Reported values are mean values of three previously developed experimental runs (data not shown)

Characterization of the PHAs obtained

The polymer obtained in fed-batch mode by applying both, the optimizing control and the exponential feeding profiles, was characterized by FTIR, ^{1}H-NMR and DSC. The spectroscopic analysis demonstrates the chemical structure of Poly(3-hydroxybutyrate) (P3HB) by reflecting the presence of the monomeric units predominantly present in PHA polymers. This result is also similar to the IR spectrum strong absorption band obtained at 1714 cm^{-1} corresponding to (C=O) ester carbonyl group, characteristics of P3HB [28].

Figure 3 shows FTIR analysis for the polymers obtained in fed-batch fermentation and for the standard from Sigma. FTIR spectra for the polymers obtained in this work show typical polyester substructures, which are very similar to the standard. The band at about 1730 cm^{-1} corresponding to the extension of C=O is wider for the case of the biopolymers obtained, which is due to the presence of a higher amount of linked carbonyls, that is, they interact forming hydrogen bridges. A band at 3450 cm^{-1} is observed corresponding to the symmetric stretching of the -OH group. The three bands

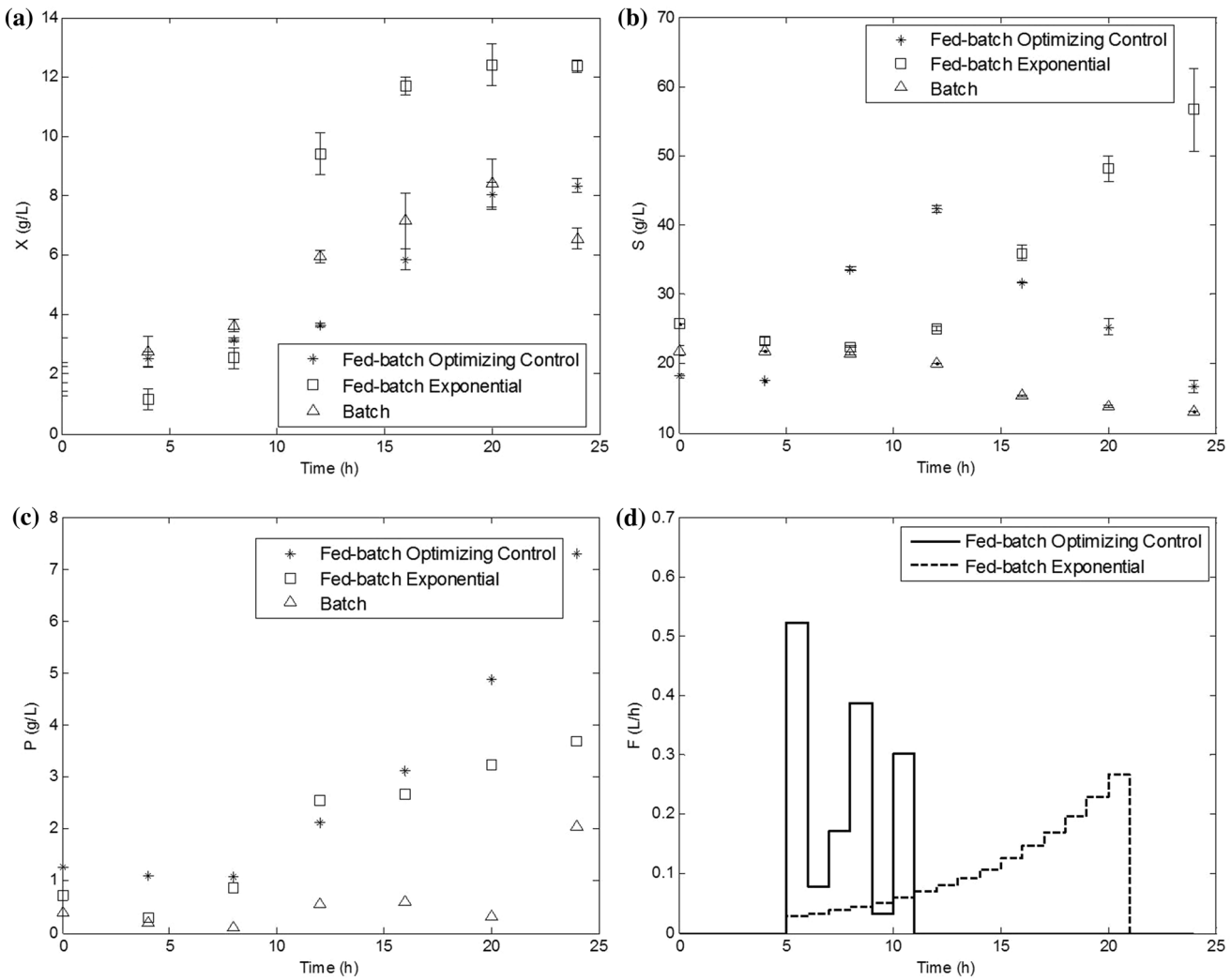

Fig. 2 Comparison of batch, fed-batch optimizing control and fed-batch exponential strategies at 5 L scale for PHA production. Results for **a** biomass, **b** substrate, **c** polymer concentration and **d** feeding profile

Table 3 Productivity and yield comparison for the different strategies

Fermentation strategy	Reaction yield (gP/gS added)	Product yield (gP/gS consumed)	Maximum PHA content (% CDW)	Productivity (g/(L h))
Batch	0.077 ± 0.0029	0.192 ± 0.0136	35%	0.088
Fed-batch-optimizing control	0.148 ± 0.0007	0.242 ± 0.0062	78%	0.27
Fed-batch-exponential	$0.050 \pm 1.79 \times 10^{-5}$	0.399 ± 0.4041	34%	0.13

at 2980, 2931 and 2914 cm^{-1} correspond to the symmetrical and asymmetric extensions of CH_2 and CH_3.

Figure 4 shows the ^{1}H-NMR spectral data of the extracted biopolymer (optimizing control and exponential, respectively) showing characteristic signals (600 MHz): d(ppm): 0.79 (m, –CH_3 HV side group), 1.21 (m, –CH_3 HB side group), 1.59 (m, –CH_2 HV side group), 2.42 (m, –CH_2 HB bulk structure), 5.18 (m, –CH HB bulk structure), respectively. The ^{1}H-NMR spectra of the PHA samples indicate that extracted intracellular compounds are similar to PHB [28]. Results shown in Fig. 4 allow concluding that the chemical structure of the biopolymer obtained using the optimizing control feed profile corresponds to the copolymer P (3HB-co-3HV). The copolymer obtained contains a

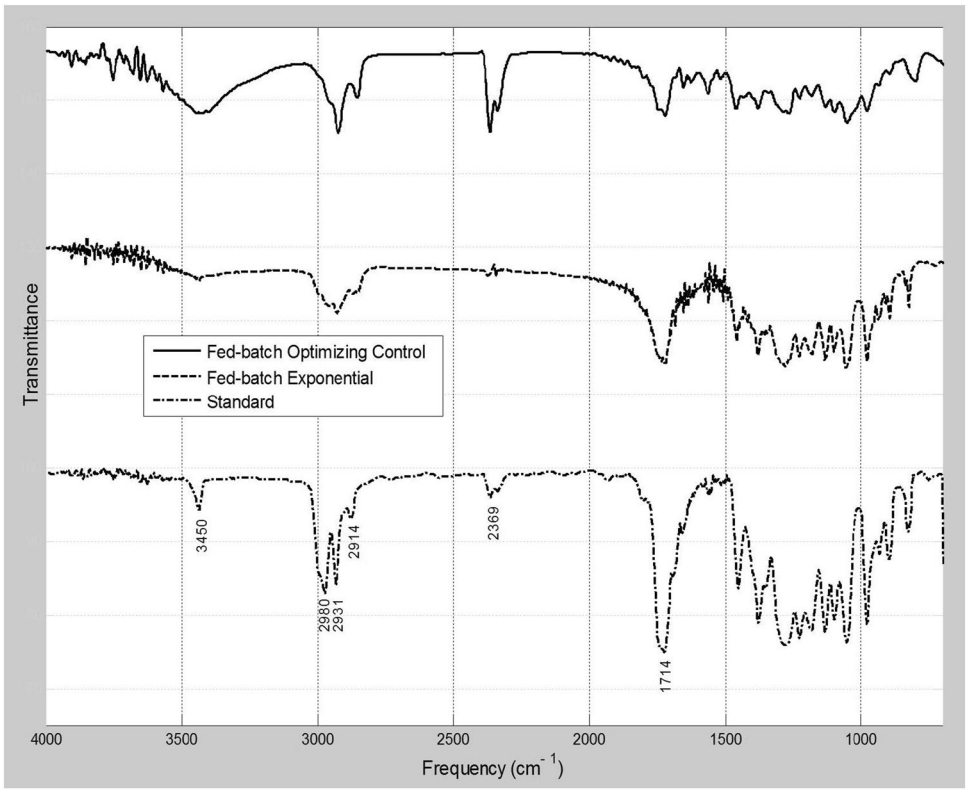

Fig. 3 FTIR spectra for the polymers obtained at fed-batch-optimizing control (top, solid line), fed-batch-exponential (middle, dashed line) and standard from Sigma (bottom, dotted-dashed line)

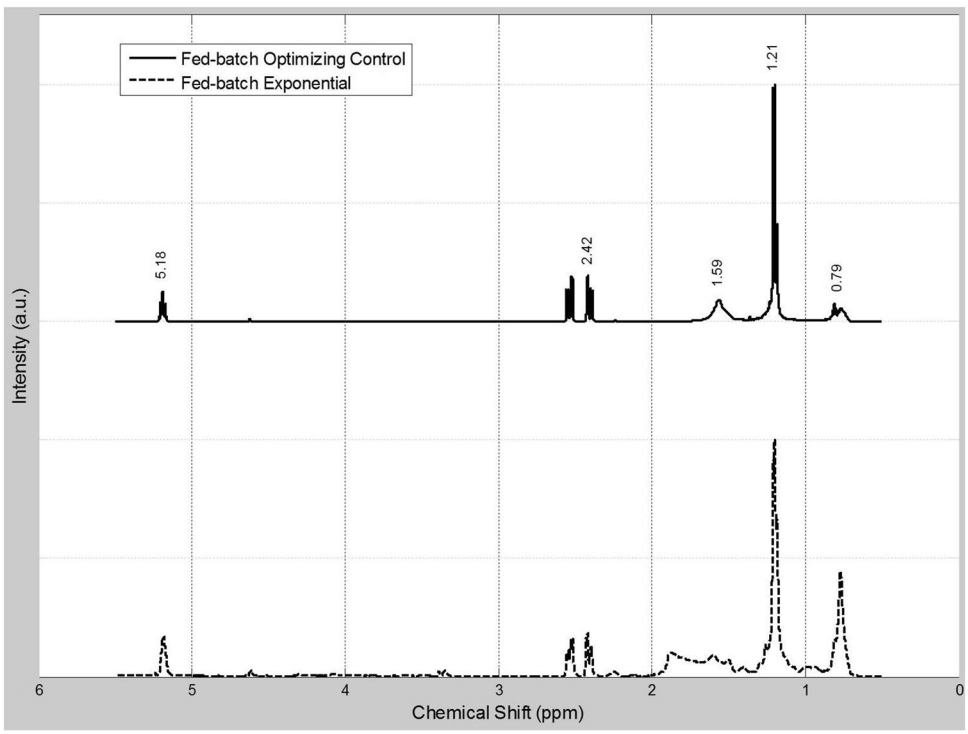

Fig. 4 ^{1}H-NMR spectra showing peaks of 3HV and 3HB side groups of PHB obtained with fed-batch-optimizing control (top, solid line) and exponential feed (bottom, dashed line)

molar fraction of monomeric units of valerate of approximately 21.6% of the polymer extracted, estimated from the ratio between the integration areas of the group $–CH_3$ for 3-hydroxyvalerate (3HV) and 3-hydroxybutyrate (3HB). Similarly, the exponential feed profile resulted in a molar percentage of 3HV of approximately 36.3%.

Table 4 and Fig. 5 summarize the results obtained by DSC for the two polymers produced by fed-batch fermentation. The glass transition temperatures (Tg) of the samples indicate that the copolymers are soft, in both cases with Tg below 0 °C. This means that at room temperature, the polymers are always in rubbery state. The expected weight composition of the copolymer can be obtained using the Fox Equation [29]:

$$\frac{1}{T_g} = \frac{w_{3HB}}{T_{g,3HB}} + \frac{w_{3HV}}{T_{g,3HV}}, \tag{16}$$

where w_{3HB} and w_{3HV} are the weight fractions of 3-hydroxybutyrate and 3-hydroxyvalerate comonomers, respectively, and $T_{g,3HB}$ and $T_{g,3HV}$ are the glass transition temperatures of the homopolymers in K. The estimated values of T_g for the homopolymers is obtained by fitting experimental data from the literature [29], resulting in: $T_{g,3HB} = 281.3$ K and $T_{g,3HV} = 229$ K. According to the Fox Equation, the polymer obtained using the optimizing control strategy resulted in a weight content of 3HV of 20.8%, corresponding to a molar content of 18.9%. Similarly, the polymer obtained using the exponential feed strategy resulted in a HV weight content of 22.5%, corresponding to a molar content of 20.5%. Thus, the slightly lower T_g of the exponential profile is probably the result of a larger presence of 3-hydroxyvalerate (3HV) in the copolymer. A result consistent with the ^{1}H-NMR analysis.

On the other hand, the melting temperature of the polymers indicates that the polymer obtained by fed-batch optimizing control had a lower melting temperature compared to the exponential feed, and both of them had lower melting points compared to that of pure PHB (~ 170–180 °C). The decrease in melting point is also the result of the presence of 3-hydroxyvalerate units in the copolymer. Interestingly, the decrease in melting point is expected to be larger for the exponential feed since the 3HV content is higher. However, the opposite is observed. Furthermore, the degree of crystallinity of the copolymers, determined as the ratio between the heat of fusion of the sample and the heat of fusion of pure PHB crystals, 146 J/g [30] indicates that the copolymer from the exponential feed presented a higher degree of crystallinity (23.8%) compared to the optimizing control feed (21.5%). These results indicate that although the optimizing control feed profile resulted in a lower content of 3HV units in the copolymer compared to the exponential feed, their configuration tend to be more random. The exponential feed, on the other hand, resulted in a more ordered structure with a higher degree of crystallinity, in spite of the higher 3HV

Table 4 Comparison of the thermal properties of the polymer obtained by the different feeding strategies

Property	PHA obtained by fed-batch-optimizing control	PHA obtained by fed-batch-exponential
T_g (°C)	−4.57	−5.6
T_m (°C)	155.07	162
ΔH_f (J/g)	31.44	34.72
Degree of crystallinity (%)	21.5	23.8

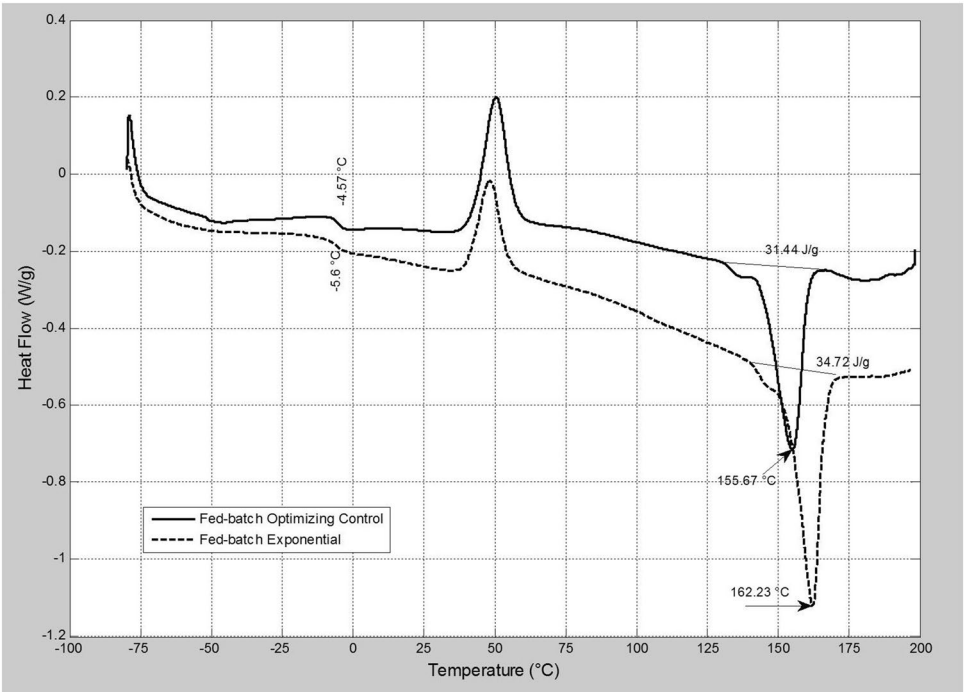

Fig. 5 DSC spectra indicating thermal stability (T_m and T_g) of PHB obtained in fed-batch by different feeding strategies: optimizing control (top, solid line), Exponential feed (bottom, dashed line)

content. Probably some segments in the copolymer obtained by exponential feeding had some sort of block copolymer configuration.

Fed-batch closed loop strategy at 500 L

As it was observed in the results shown in Table 3, although the fed-batch-optimizing control has shown better results in comparison to the batch process (as it was expected), the actual improvements did not outperform the batch results in terms of yield and productivity. Therefore, in an attempt to improve the process yield and productivity, the incorporation of a closed loop control strategy for keeping the substrate concentration at a constant value during fed-batch operation is proposed. The closed loop strategy relies upon online information for biomass and substrate concentrations, which is provided by two soft-sensors developed in this work. The two sensors are simple models (software) that just require online measurements for O_2 and CO_2 at the exhaust gas (hardware). Therefore, implementation of these soft-sensors might be convenient for industrial implementation. In this section, it will be first shown the development of the soft-sensors. Then, results for the closed loop strategy applied in a 500-L fermenter are presented.

Soft-sensors development

It is well known that one of the main drawbacks in bioprocess operation is the absence of reliable and cheap sensors that allow monitoring online important variables such as biomass, substrate or metabolites' concentration [31]. Soft-sensors have been used as an alternative but they are usually based on complex models, or they require additional expensive tools (software and hardware) for their implementation. Generally speaking, a soft-sensor (or software sensor) is a model whose predictions combine the use of software (for simulating the model) with information from available sensor measurements. Soft-sensors are used for estimating in real time, process variables that are not available (or that are difficult) of being measured online. It is important to notice that the success of a soft sensor relies upon two main things. First, the traditional sensors (hardware) must provide reliable measurements of the output variables required for predicting the unmeasured variable. Second, the estimator (software) used should be a model able to predict online and with an expected accuracy, the actual values of the desired state variables [32].

In this section, the development of simple but effective soft-sensors for biomass and sugar concentration prediction is explained. The soft sensors developed use as online information, only the O_2 and CO_2 values measured by a BlueInOne Cell exit gas analyzer (BlueSens, Herten, Germany).

Assuming that oxygen uptake is carried out for biomass growth and cell maintenance, from a total mass balance for oxygen, we have:

$$\frac{\mathrm{d}\left(VO_{2L}\right)}{\mathrm{d}t} = \dot{m}_{O_{2in}} - \dot{m}_{O_{2out}} - \dot{m}_{O_{2growth}} - \dot{m}_{O_{2maint.}}, \tag{17}$$

where $\dot{m}_{O_{2in}}$ and $\dot{m}_{O_{2out}}$ are the input and output mass flow of oxygen, respectively. $\dot{m}_{O_{2growth}}$ and $\dot{m}_{O_{2maint.}}$ represent the oxygen uptake for cellular growth and maintenance, respectively. Each term in Eq. (17) is given by:

$$\dot{m}_{O_{2in}} - \dot{m}_{O_{2out}} = \frac{\left(\%O_{2in} - \%O_{2out}\right)F_{air}\,\rho_{O_2}\,Y_{X/O_2}}{100\%\,V}, \tag{18}$$

$$\dot{m}_{O_{2growth}} = \frac{1}{Y_{X/O_2}}\frac{\mathrm{d}(VX)}{\mathrm{d}t}, \tag{19}$$

$$\dot{m}_{O_{2maint.}} = \frac{X\,V\,Y_m}{Y_{X/O_2}}, \tag{20}$$

where $\%O_{2in}$ and $\%O_{2out}$ are the oxygen percentage at the air and the oxygen percentage detected by the sensor at the exhaust gas. F_{air} is the air volumetric flowrate fed to the process (which is kept constant), ρ_{O_2} and Y_{X/O_2} are the oxygen density and the yield coefficient for biomass from oxygen, respectively. V is the culture volume and Y_m is the maintenance rate for consumption of oxygen. Assuming that the oxygen concentration is kept constant at a predefined setpoint (i.e. thanks to a dissolved oxygen concentration control loop), we arise to the soft-sensor equation for predicting the changes in biomass concentration:

$$\frac{\mathrm{d}X}{\mathrm{d}t} = \frac{\left(\%O_{2in} - \%O_{2out}\right)F_{air}\,\rho_{O_2}\,Y_{X/O_2}}{100\%\,V} - XY_m - \left[\frac{X}{V} + \frac{O_{2L}Y_{X/O_2}}{V}\right]\frac{\mathrm{d}V}{\mathrm{d}t}. \tag{21}$$

On the other hand, from a mass balance for the substrate, we have

$$\frac{\mathrm{d}(VS)}{\mathrm{d}t} = FS_{in} - r_s V, \tag{22}$$

where the first term corresponds to the mass flow of substrate entering into the bioreactor by the feedflow, and the second term represents the substrate consumed. F is the substrate feed rate, S_{in} is the substrate concentration in the feed and r_s is the substrate consumption rate. When sugars are consumed (for both biomass and polymer production), CO_2 is produced. Therefore, the substrate consumption term will be related to the carbon dioxide detected at the exhaust gas, as follows:

$$r_s V = \frac{\%CO_{2out}\ F_{air}\ \rho_{CO_2}}{100\%\ \ Y_{CO_2/S}}, \tag{23}$$

where $\%CO_{2out}$ is the CO_2 percentage at the exhaust gas, ρ_{CO_2} and $Y_{CO_2/S}$ are the CO_2 density and the yield coefficient for CO_2 from substrate, respectively. Therefore, the soft-sensor equation for predicting the dynamic behaviour for the substrate concentration is:

$$\frac{dS}{dt} = \frac{FS_{in}}{V} - \frac{\%CO_{2out}\ F_{air}\ \rho_{CO_2}}{100\%\ \ Y_{CO_2/S}\ V} - \frac{S}{V}\frac{dV}{dt}. \tag{24}$$

Table 5 reports the value for the parameters used in the soft-sensors calculations. Yield values were determined by minimizing the error between the experimental data and soft-sensor predictions.

Validation of the soft-sensors was carried out using the data reported before for the fed-batch experiments at 5 L bioreactor. Figure 6a, b shows the comparison between the experimental data and the soft-sensor predictions for biomass and substrate concentrations, respectively, for the case in which fed-batch fermentation was carried out by implementing the feeding profile given by the optimizing control. Figure 6c, d shows the comparison between the experimental data and the soft-sensor predictions for the substrate concentration for the case in which the exponential feeding profile was applied.

As it can be seen in Fig. 6a, c, biomass predictions by the soft-sensor proposed in this work (Eq. 21) results in a good agreement with the experimental data. The root mean square error (RMSE) obtained for the biomass predictions is 0.611 g/L and 1.026 g/L, for the cases in Fig. 6a, c, respectively. On the other hand, substrate predictions by the soft-sensor (Eq. 24) presented a good agreement with the experimental data during the initial batch operation and the fed-batch stage. However, after starting the second and final batch stage, predictions presented considerable deviations. This last fact could suggest the need of re-tuning some of the soft-sensor parameters after finishing the fed-batch stage.

Table 5 Parameters used in the soft-sensors

Parameter[a] (units)	Description	Value
ρ_{O_2} (g/L)	Oxygen density	1.331
Y_{X/O_2} (gX/gO_2)	Yield coefficient for biomass from oxygen	0.921
Y_m (h^{-1})	Maintenance rate for consumption of oxygen	0.0415
ρ_{CO_2} (g/L)	Carbon dioxide density	1.842
$Y_{CO_2/S}$ (gCO_2/gS)	Yield coefficient for CO_2 from substrate	1.240

[a]Reported values are mean values of three previously developed experimental runs (data not shown)

Despite such deviations, it is worth emphasizing that substrate predictions during the most important process stages has been successfully. The RMSE for the substrate predictions is 6.27 g/L and 6.79 g/L for the cases in Fig. 6b, d, respectively.

Experimental implementation of a closed-loop control strategy at 500 L scale

After validating the soft-sensors for online prediction of the biomass and substrate concentrations, a closed loop control strategy for keeping the substrate concentration at a pre-defined value during fed-batch operation was implemented at 500 L scale. Figure 7 shows a block diagram for the closed-loop control strategy applied.

As it can be seen in Fig. 7, the implemented strategy is a feedback loop for keeping the substrate concentration at a desired set-point (S_{sp}). However, it must be noticed that this strategy is designed for being applied only during fed-batch operation. The controller equation for calculating the flow rate required for keeping the substrate at the set-point has been derived from the unstructured model presented in Eqs. (2)–(8), specifically from Eq. (4), re-named here as Eq. (25).

$$\frac{dS}{dt} = -C_{sx}\mu X - R_{csx}X - C_{sp}\left(K_1\mu X + K_2 X\right) + \frac{F}{V}S_{in} - \frac{F}{V}S, \tag{25}$$

where μX is taken from Eq. (3) as:

$$\mu X = \frac{dX}{dt} + \frac{F}{V}X, \tag{26}$$

and the term $\frac{dS}{dt}$ is approximated as

$$\frac{dS}{dt} \approx \frac{\Delta S}{\Delta t} = \frac{S_{sp} - S(t-\Delta t)}{\Delta t}, \tag{27}$$

where S_{sp} and $S(t-\Delta t)$ are the defined set-point for the substrate concentration and the substrate concentration at the previous sample time, respectively. Furthermore, Δt is the sample time. Finally, replacing Eqs. (26) and (27) in Eq. (25) and solving for F, the controller equation is obtained:

$$F = \frac{V\left[\frac{dX}{dt}\left(C_{sx} + C_{sp}K_1\right) + X\left(R_{csx} + C_{sp}K_2\right) + \frac{\left(S_{sp} - S(t-1)\right)}{\Delta t}\right]}{S_{in} - S - X\left(C_{sx} + C_{sp}K_1\right)}. \tag{28}$$

As mentioned, the closed loop control strategy proposed intends to keep the substrate concentration at a constant value (S_{sp}), during fed-batch operation. In this work, the set point value was defined to be 15.2 g/L (2 g per liter under the initial substrate concentration). Furthermore, the fed-batch stage was started after allowing a batch period of 10 h. Figure 8 shows the dynamic behaviour of the main process state

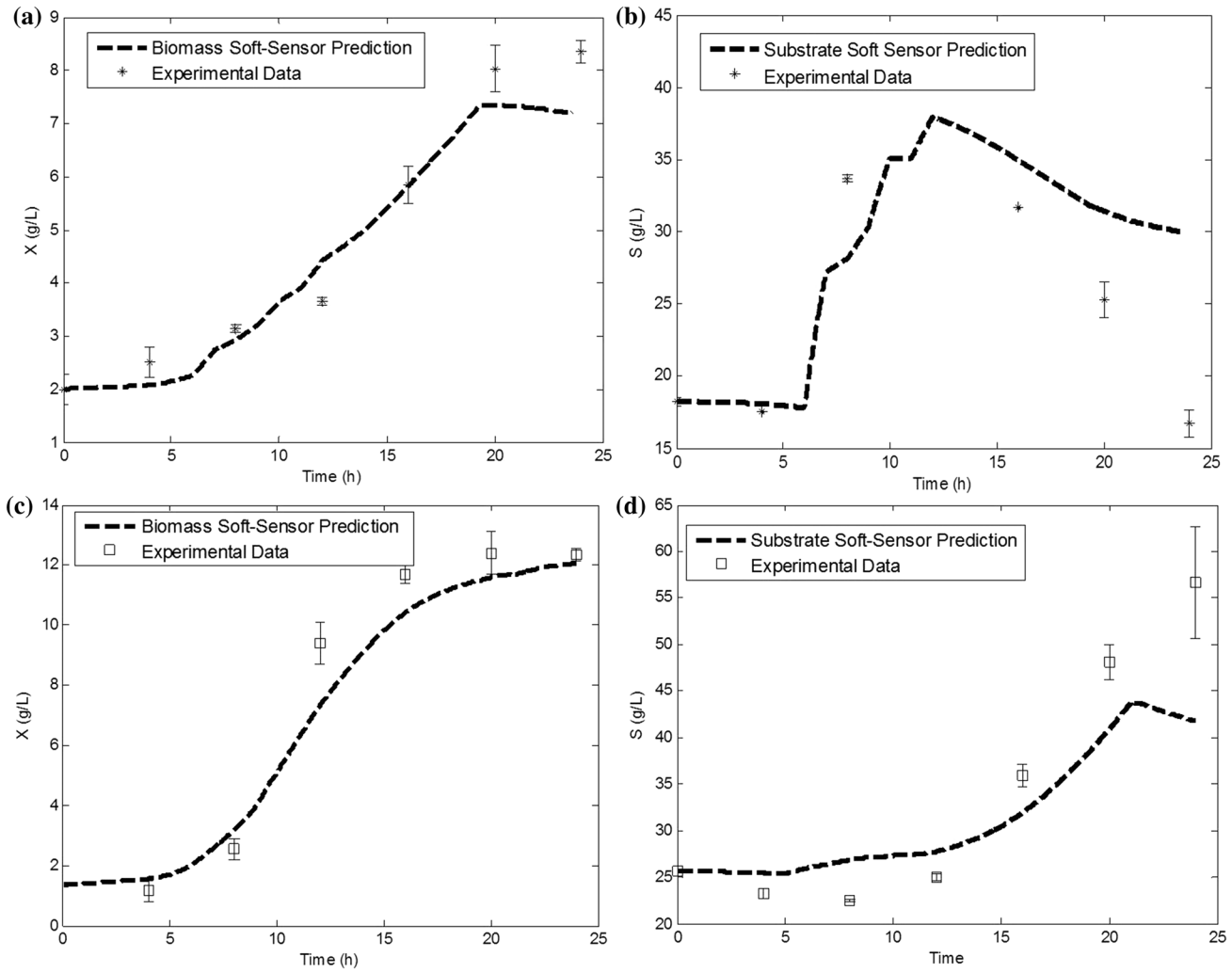

Fig. 6 Soft-sensor validation: comparison between experimental data and the soft-sensor predictions for biomass and substrate. **a** Biomass and **b** substrate at the fed-batch optimizing control case. **c** Biomass and **d** substrate at the exponential feeding profile case

variables when the closed control loop for keeping constant the substrate concentration was implemented.

Figure 8a shows the substrate, both, predicted by the soft sensor and the actual experimental value. It is worth reminding that the control law was applied only by using the soft-sensor information and that the controller was set on only after 10 h of a batch period. At that time, the substrate concentration predicted by the soft-sensor was around 12 g/L (3 g/L under the set-point). Therefore, when the controller was set on, it calculated immediately the required feed flow for increasing the substrate concentration and kept doing so after the final process time (24 h). Figure 8b shows the feeding profile calculated by the controller (Eq. 28). Although the online-predicted substrate concentration did not exactly match the set-point, it is possible to observe that the controller has a good performance. For 14 h of fed-batch operation, the RMSE is 1.28 g/L, with a minimal error value of 0.56 g/L and a maximal error of 3.17 g/L (this last value is the error at the first time instant when the controller was set on). On the other hand, Fig. 8c shows the biomass dynamic behaviour, where it is possible to observe a good agreement between the experimental data and the soft-sensor predictions for around 15 h. Then, predictions start deviating from the actual value (something similar is observed for the substrate predictions). The reason for such deviations is that in the derivation of the soft-sensors, all model parameters were considered as constants. However, it is known that some parameters (i.e. the specific growth rate and the yields) are time-varying parameters. Therefore, as mentioned before, this could suggest that some model parameters should be re-identified after some time, in order to update such information in the soft-sensors. Finally, Fig. 8d shows the dynamic behaviour for the polymer. As it is seen, polymer concentration just reached around 1.2 g/L after 24 process hours.

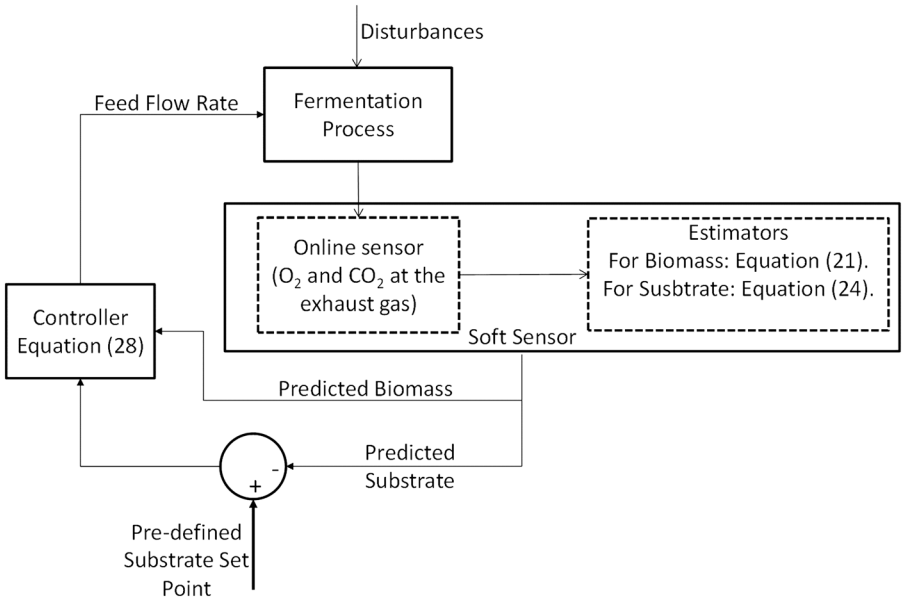

Fig. 7 Closed loop control strategy based on biomass and substrate soft-sensors

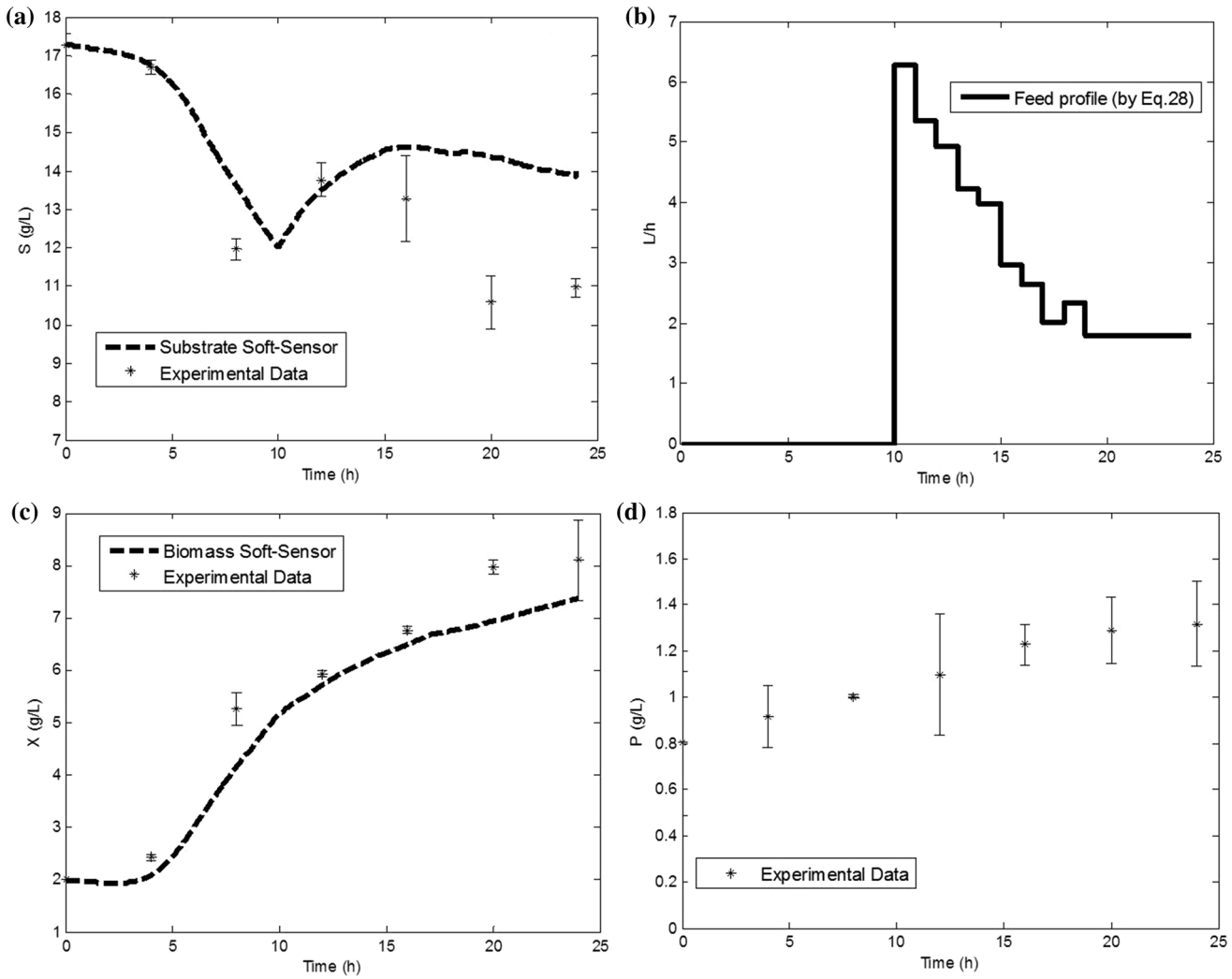

Fig. 8 Closed loop control strategy results: **a** substrate (predicted vs. actual), **b** feed profile, **c** biomass (predicted vs. actual) and **d** polymer

Of course, this is not a good result because it is lower than the obtained at the batch process at 5 L scale. However, the main point here was to show the implementation of the closed loop control strategy based on the developed soft-sensors. Currently, scaling factors that could have affected the polymer production at the 500-L scale are under analysis, in order to improve the process operation at this scale.

Conclusions

Process System Engineering Tools have been applied for both, laboratory (5 L) and pilot plant (500 L) scale fed-batch production of Poly(3-hydroxybutyrate-*co*-3-hydroxyvalerate), using a vinasses–molasses mixture. On-line estimation for biomass and substrate was possible by applying the first-principles-based soft-sensors developed in this work, which only require measuring the O_2/CO_2 content at the exhaust gas. Successful validation of the soft-sensors was carried out against experimental data at 5 L scale. On the other hand, a model-based closed loop control strategy for achieving a constant pre-defined substrate concentration (set-point) was derived and implemented at 500 L scale. Substrate concentration predicted by the soft-sensor was used as the "measured" process variable, for determining the feeding profile required for keeping constant the set-point. This implementation allowed the control of the substrate concentration during 14 h of operation. Results of the implemented control loop were confirmed by comparing against offline measurements of the sugars' concentration. Although the concentration of polymer obtained in these experiments was relatively low compared to the best values reported in the literature, it can be concluded that the proposed control loop strategy is worthy of implementation because, at a low cost, it can be used for keeping the substrate concentration at a predefined set point. On the other hand, it was shown that by applying different feeding strategies, the characteristics of the obtained product vary. Therefore, in order to assure the desired end-product characteristics, a control strategy combining the soft-sensors developed in this work, with soft-sensors capable of predicting end-product properties, might be a powerful strategy for being implemented at industrial level in order to strengthen the economic feasibility of the biopolymers industry.

Acknowledgements Financial support from COLCIENCIAS through the research project with contract number FP44842-064-2015 is gratefully acknowledged. Authors gratefully acknowledge the support given by the research group Laboratorio de Investigación en Polímeros at University of Antioquia, where the polymer characterization was carried out.

Compliance with ethical standards

Conflict of interest The authors declare no conflict of interest.

References

1. Ntaikou I, Koumelis I, Tsitsilianis C, Parthenios J, Lyberatos G (2018) Comparison of yields and properties of microbial polyhydroxyalkanoates generated from waste glycerol based substrates. Int J Biol Macromol 112:273–283
2. Nielsen C, Rahman A, Rehman AU, Walsh MK, Miller CD (2017) Food waste conversion to microbial polyhydroxyalkanoates. Microbial Biotechnol 10(6):1338–1352
3. Salakkam A, Webb C (2018) Production of poly (3-hydroxybutyrate) from a complete feedstock derived from biodiesel by-products (crude glycerol and rapeseed meal). Biochem Eng J 137:358–364
4. Bhattacharyya A, Pramanik A, Maji SK, Haldar S, Mukhopadhyay UK, Mukherjee J (2012) Utilization of vinasse for production of poly-3-(hydroxybutyrate-*co*-hydroxyvalerate) by *Haloferax mediterranei*. AMB Express 2(1):34
5. Pramanik A, Mitra A, Arumugam M, Bhattacharyya A, Sadhukhan S, Ray A et al (2012) Utilization of vinasse for the production of polyhydroxybutyrate by *Haloarcula marismortui*. Folia Microbiol 57(1):71–79
6. Khanna S, Srivastava AK (2006) Optimization of nutrient feed concentration and addition time for production of poly (β-hydroxybutyrate). Enzyme Microbial Technol 39(5):1145–1151
7. López JA, Bucalá V, Villar MA (2010) Application of dynamic optimization techniques for poly (β-hydroxybutyrate) production in a fed-batch bioreactor. Indus Eng Chem Res 49(4):1762–1769
8. Lopez-Arenas T, González-Contreras M, Anaya-Reza O, Sales-Cruz M (2017) Analysis of the fermentation strategy and its impact on the economics of the production process of PHB (polyhydroxybutyrate). Comput Chem Eng 107:140–150
9. Penloglou G, Vasileiadou A, Chatzidoukas C, Kiparissides C (2017) Model-based intensification of a fed-batch microbial process for the maximization of polyhydroxybutyrate (PHB) production rate. Bioprocess Biosyst Eng 40(8):1247–1260
10. Novak M, Koller M, Braunegg M, Horvat P (2015) Mathematical modelling as a tool for optimized PHA production. Chem Biochem Eng Q 29(2):183–220
11. Moran-Salazar RG, Sanchez-Lizarraga AL, Rodriguez-Campos J, Davila-Vazquez G, Marino-Marmolejo EN, Dendooven L, Contreras-Ramos SM (2016) Utilization of vinasses as soil amendment: consequences and perspectives. SpringerPlus 5(1):1007
12. Christofoletti CA, Escher JP, Correia JE, Marinho JFU, Fontanetti CS (2013) Sugarcane vinasse: environmental implications of its use. Waste Manage 33(12):2752–2761
13. Ortegón GP, Arboleda FM, Candela L, Tamoh K, Valdes-Abellan J (2016) Vinasse application to sugar cane fields. Effect on the unsaturated zone and groundwater at Valle del Cauca (Colombia). Sci Total Environ 539:410–419
14. Moraes BS, Triolo JM, Lecona VP, Zaiat M, Sommer SG (2015) Biogas production within the bioethanol production chain: use of co-substrates for anaerobic digestion of sugar beet vinasse. Bioresour Technol 190:227–234
15. Acosta-Cárdenas A, Alcaraz-Zapata W, Cardona-Betancur M (2018) Sugarcane molasses and vinasse as a substrate for polyhydroxyalkanoates (PHA) production. DYNA 85(206):220–225
16. Pant D, Adholeya A (2007) Biological approaches for treatment of distillery wastewater: a review. Bioresour Technol 98(12):2321–2334
17. Escalante-Sánchez A, Barrera-Cortés J, Poggi-Varaldo HM, Ponce-Noyola T, Baruch IS (2018) A soft sensor based on online biomass measurements for the glucose estimation and control of fed-batch cultures of Bacillus thuringiensis. Bioprocess Biosyst Eng 41(10):1471–1484

18. Mears L, Stocks SM, Sin G, Gernaey KV (2017) A review of control strategies for manipulating the feed rate in fed-batch fermentation processes. J Biotechnol 245:34–46
19. Oliveira R, Simutis R, de Azevedo SF (2004) Design of a stable adaptive controller for driving aerobic fermentation processes near maximum oxygen transfer capacity. J Process Control 14(6):617–626
20. Srinivasa BB, Moreshwar JM (2009) U.S. Patent Application No. 12/349,134
21. Pagliano G, Ventorino V, Panico A, Pepe O (2017) Integrated systems for biopolymers and bioenergy production from organic waste and by-products: a review of microbial processes. Biotechnol Biofuels 10(1):113
22. Aramvash A, Moazzeni Zavareh F, Gholami Banadkuki N (2018) Comparison of different solvents for extraction of polyhydroxybutyrate from *Cupriavidus necator*. Eng Life Sci 18(1):20–28
23. Heinrich D, Madkour MH, Al-Ghamdi MA, Shabbaj II, Steinbüchel A (2012) Large scale extraction of poly (3-hydroxybutyrate) from *Ralstonia eutropha* H16 using sodium hypochlorite. AMB Express 2(1):59
24. Amicarelli A, Quintero O, di Sciascio F (2014) Behavior comparison for biomass observers in batch processes. Asia-Pacific J Chem Eng 9(1):81–92
25. Chatzidoukas C, Penloglou G, Kiparissides C (2013) Development of a structured dynamic model for the production of polyhydroxybutyrate (PHB) in Azohydromonas lata cultures. Biochem Eng J 71:72–80
26. Ochoa S (2016) A new approach for finding smooth optimal feeding profiles in fed-batch fermentations. Biochem Eng J 105:177–188
27. Mozumder MSI, De Wever H, Volcke EI, Garcia-Gonzalez L (2014) A robust fed-batch feeding strategy independent of the carbon source for optimal polyhydroxybutyrate production. Process Biochem 49(3):365–373
28. Mohapatra S, Mohanta PR, Sarkar B, Daware A, Kumar C, Samantaray DP (2017) Production of polyhydroxyalkanoates (PHAs) by Bacillus strain isolated from waste water and its biochemical characterization. Proc Natl Acad Sci India Sect B Biol Sci 87(2):459–466
29. Avella M, Martuscelli E, Raimo M (2000) Review properties of blends and composites based on poly (3-hydroxy) butyrate (PHB) and poly (3-hydroxybutyrate-hydroxyvalerate)(PHBV) copolymers. J Mater Sci 35(3):523–545
30. Kulkarni SO, Kanekar PP, Nilegaonkar SS, Sarnaik SS, Jog JP (2010) Production and characterization of a biodegradable poly (hydroxybutyrate-*co*-hydroxyvalerate)(PHB-co-PHV) copolymer by moderately haloalkalitolerant Halomonas campisalis MCM B-1027 isolated from Lonar Lake, India. Bioresour Technol 101(24):9765–9771
31. Veloso AC, Ferreira EC (2017) Online analysis for industrial bioprocesses: broth analysis. In: Larroche C, Ángeles Sanromán M, Du G, Pandey A (eds) Current developments in biotechnology and bioengineering. Elsevier, Amsterdam, pp 679–704
32. Chéruy A (1997) Software sensors in bioprocess engineering. J Biotechnol 52(3):193–199